Bridging the lesioned spinal cord using hydrogel

By

Le Thi Anh Hong

Major in Neurosciences

Department of Biomedical Science

The Graduate School, Ajou University

Bridging the lesioned spinal cord using hydrogel

by

Le Thi Anh Hong

Dissertation Submitted to The Graduate School of Ajou University

in Partial Fulfillment of The Requirements for the Degree of

Master of Biomedical Science

Supervised by

Byung Gon Kim, MD, PhD.

Major in Neurosciences

Department of Biomedical Science

The Graduate School, Ajou University

June, 2015

This Certifies that the dissertation

of Le Thi Anh Hong is approved.

SUPERVISORY COMMITTEE

_____

Eun Hye Joe

_____

Byung Gon Kim

_____

Eunn Young Kim

The Graduate School, Ajou University

June 26th, 2015

- ABSTRACT -

Bridging the lesioned spinal cord using hydrogel

Spinal cord injury (SCI) results in permanent functional deficits due to disruption of axonal connections. Attempts to repair injured spinal cord have been focused on axon regeneration in order to re-establish connections between the brain and the spinal cord below the injury level. Contusive injury, which is the most frequent type of injury occurring in human patients, leads to a formation of cystic cavities at the lesion epicenter. The cavity formation is one of major obstacles for axonal regeneration since injured axons fail to reach caudal tissue in the absence of physical and mechanical supports from extracellular matrix (ECM). Implanting artificial scaffolds has been proposed as a promising approach, but successful bridging with scaffolding biomaterials has not been convincingly demonstrated in clinically relevant contusive SCI model. Unpredictable and irregular geometry of lesion cavities formed in this model would necessitate the use of injectable hydrogel for this purpose. In the present study, I injected temperature sensitive poly(phosphazene) hydrogel, with a sol-gel transition behavior at 37℃, into the lesion epicenter in contusive rat SCI model at 1 week after injury. The hydrogel injection almost completely prevented cavity formation. In animals with the hydrogel injection, the lesion epicenter was replaced by fibronectin (FN)-enriched ECM by 4 weeks after the injection. The FN-positive ECM was surrounded by GFAP positive glial scars with an interface laden with chondroitin sulfate proteoglycans. Injection of hydrogel mixed with Taxol, which was previously reported to selectively suppress fibrotic scars, resulted in the failure of bridging cavities, suggesting a role of ECM produced by fibroblasts in the hydrogel effects. Interestingly, zymography showed upregulation of MMP-9 activity in animals with the hydrogel injection, and MMP-9 was highly expressed at the center of the FN-enriched ECM. The cellular source for the MMP-9 immunoreactivity was CD11b positive macrophages. Co-localization of FN and collagen-1Ŭ1 suggested that the majority of th

perivascular fibroblasts.Animals with hydrogel injection showed improvement in coordinated locomotion as evidenced by BBB test and Catwalk analysis. The improvement in locomotor function was accompanied by better preservation of myelinated white matter around the lesion epicenter. Our study establishes a proof of principle that the temperature-sensitive hydrogel can be used as a cavity-bridging therapy for contusive SCI. Considering the versatility of hydrogel in a sol state incorporating various drugs and cells, this approach can also be utilized as a platform for multifaceted combinatorial therapy.

TABLE OF CONTENTS

LIST OF FIGURES

ABBREVIATION

BBB: Blood brain barrier

CD11b: intergrin, alpha M

CD68: Cluster of Differentiation 68

Col1Ŭ1: Collagen 1Ŭ1

CSPG: Chondroitin sulfate proteoglycan

ECM: Extracellular matrix

FN(+): Fibronectin positive

GFAP: Glial fibrillary acidic protein

HA: Hyaluronan

Iba1: Ionzied calcium binding adaptor molecule 1

MMP-2: Matrix metalloproteinase 2

MMP-9: Matrix metalloproteinase 9

PBS: Phosphate buffered saline

PDGFR-ϐ Platelet-derived growth factor receptor- beta

SCI: Spinal cord injury

I. INTRODUCTION

A. Spinal Cord Injury

Patients with spinal cord injury (SCI) suffer from life-long permanent deficits in neurological functions. Injuries occurring at high levels such as cervical injury usually lead to more severe deficits involving 4 limbs and respiration than those in lower levels of spinal cord resulting in paraplegia. Costs for care and treatment in patients with SCI is enormously huge ($3 billion each year in America) (http://www.ninds.nih.gov/disorders/sci/detail_sci.htm). Not only does SCI cause patients themselves poor quality of life but also create economic burdens for their family and the society they belong to. The most common cause of SCI is traffic accident, besides falling, sport-related injuries, violence, and others. Among various type of injury, contusion injury is the most popular form of injury, accounting for more than 60% of SCIs (Macaya and Spector, 2012). In contusion injury, mechanical forces by compression with displaced vertebral bones are rapidly inflicted upon the spinal cord, leading to disorganization of spinal cord tissue. Although most of axons in the affected area are severed in the lesion epicenter, a certain extent of viable and intact axons are still observed at the injury site depending on the degree of injury.

Until present, there is no effective therapeutic strategy to treat SCI. Incomplete injury results in axonal disruption accompanied by damages to the remaining white matter. Attempts to repair SCI have been centered on axon regeneration to reestablish the lost connections between the brain and the nerve below the injury site. Not only do injured axons in center nervous system (CNS) have low capacity to regrowth but also hostile environment after injury inhibit their regeneration. Thus, effective treatment of SCI leading to function recovery would ultimately require multifaceted strategies. SCI triggers a series of molecular and cellular alternations resulted in cystic cavities formation (Fitch et al., 1999). In human contusive SCI, a cystic cavity was observed, and a similar pattern of cavity formation was seen in rat contusive injury while cavity does not form after mice SCI. The exact mechanism why cystic cavities develop in contusive injury still remains to be elucidated.

B. Cavity formation and the importance of bridging lesion after spinal cord injury.

In CNS, ECM acts as a framework that supports cell migration, synaptogenesis, and axonal guidance during development. Components of ECM change dynamically in shape and design in response to alterations of environment. ECM found in CNS is rich in proteoglycans and glycoproteins that are attached in hyaluronic acid (HA). Particularly, sulphated proteoglycans attached to tenascins and linked with HA by link proteins are densely distributed in intercellular spaces, or accumulated into condensed structures which cover presynaptic nerve terminal, surrounds perineuronal nets (PNNs) and node of Ranvier. ECM has vital role in regulating important molecular and cellular activities in physical condition (Burnside and Bradbury, 2014). However, following injury, the composition and expression of ECM proteins are changed and the alternations of ECM following injury can have unfavorable ramifications on neural repair.

Primary damages from physical injury are comprised of hemorrhage, ischemia, and unbalanced ionic homeostasis, and so forth. The primary insult is followed by secondary degenerative processes. For example, inflammatory cells infiltrate into the lesion site eliciting cellular demise via apoptosis or necrosis. Oligodendrocytes in the remote white matter are also susceptible to delayed death, contributing to demyelination and degeneration of the white matter (El Waly et al., 2014). One of the consequences of the secondary degenerative processes is a formation of fluid-filled cavity. Exact mechanisms by which cystic cavities develop following contusion injury remain to be clarified. It is hypothesized that post injury inflammatory reactions activate matrix remodeling enzymes, which in turn degrade ECM proteins leading a formation of cystic spaces (Fitch et al., 1999). Several studies have investigated mechanism of cavity formation. It was shown that inflammation alone can trigger secondary tissue damage culminating in cavitation. In addition, disruption of vascular supply may exacerbate cavitation process (Rooney et al., 2009), however the question of how this cavity develop remains largely unknown.

The expansion of cystic cavities are inevitably associated with disruption of passing axons and further loss of glial cells and spinal neurons in the parenchyma. The cavities are usually surrounded by astrocytic glial scars and chondroitin sulfate proteoglycan (CSPG) produced from them, which are known to potently impede axon regeneration (Kwok et al., 2008). More importantly, injured axons would have great difficulty in growing within fluid

filled cavities due to the lack of mechanical and physical supports from ECM proteins. Therefore, the formation of cystic cavities presents an onerous challenge not only for prevention of secondary damage but also for inducing regeneration of axon. There was an attempt to attenuate necrosis aiming at reducing cavity formation without a meaningful success (Fujiki et al., 2004). I speculate that developing effective strategies to prevent cavity formation or to provide bridging materials to fill the cavity spaces would be imperative for patients with spinal cord injury.

C. Bridging cavity using biomaterials

Various biomaterials have been used in past decades aiming at bridging the lesion cavity and thus at constituting extracellular matrix framework for the support of axon growth. Basically, they can be classified following their physical or chemical properties including natural or artificial scaffolds, solid or injectable, biodegradable or non-degradable materials (reference should be added). Biomaterials that are suited for being implanted into lesioned spinal cord should have certain properties for ideal outcomes. One of the important properties is biocompatibility with the host tissue. It is important not to elicit any immune reaction or produce toxic effects on host tissue or cells over a long period of time. Biomaterials also should not produce further damage when being introduced to the spinal cord. In this regard, being injectable rather solid would be advantageous since injectable hydrogel would not require surgical procedure for implantation. Last but not least, biomaterials should be degraded at the same time of tissue formation otherwise it may be toxic and become barrier for tissue regeneration. On the contrary, earlier degradation than necessary may cause tissue shrinkage and structural collapse, increase inflammation and scarring (Sung et al., 2004). Therefore, many studies have focused on using biodegradable scaffolds. (Friedman et al., 2002; Tabesh et al., 2009), chitosan (Nomura et al., 2008; Zahir et al., 2008), collagen (Paino and Bunge, 1991) and poly(L-lactide) are typical natural degradable materials. Time course of tissue formation and degradation rate has not been well characterized. At least in rodents, however, degradation rates on the order of weeks to months would be considered adequate because axonal growth and tissue regeneration are thought to occur with a time course ranging from three weeks to three months after injury (Mahoney and Anseth, 2006).

While natural scaffolds are expected to minimize immune rejection, artificial biomaterials have advantages of being readily modified by changing their physical and chemical properties. In addition, artificial scaffold can be synthetized in a large amount. Scaffolding biomaterials are being sought for biomedical application not only for their physical effects of filling for tissue defect but also to carry certain growth factors, therapeutic cells, drugs and so on (Woerly et al., 2001a; Woerly et al., 2001b). Previously, solid scaffold was used in hemi section spinal cord injury model (Teng et al., 2002). In this study, scaffold was fabricated before creating hemisected or transected injury model and spinal cord segment was dissected following exactly same size and morphology of scaffold. There were also a lot of studies that used scaffolds to bridge the lesion gaps in transection model. Spinal cord was completely transected and scaffolds were used to connect rostral and caudal stumps (Gao et al., 2013; Tsai et al., 2004). This kind of model has advantage of making sure that regenerating axons that found after implantation, originate from injured axons rather than spared axons. Although it was successful to implant scaffolds to injury site and functional recovery was observed in some degree but hemisection or transection injury model are not clinical relevant since majority of human injury occurs in contusion type. Unlike transection or hemisection injury, contusive injury would lead to a formation of cavities of unpredictable shape and geometry. Being injectable, therefore, would be a particularly critical quality for considering scaffolding biomaterials in contusion injuries. Moreover, implantation of solid framework into human spinal cord is unnatural and may pose unpredictable risks. Solid scaffold is disadvantageous also because it is hard to handle and to load peptides or drugs Furthermore, solid nature may not create good distribution network that necessary for cells, peptides, drugs, trophic factors infiltration within it. Injectable hydrogel would be an advanced material to meet these challenges.

D. Injectable hydrogel for contusive injury model

A various number of injectable materials have been produced for a variety of tissue specific applications not only for brain and spinal cord but also bone, cartilage, intervertebral disk (Kretlow et al., 2007). Hydrogels are cross-linked polymers with hydrophilic properties. They have tissue like water content, porous structure pore size 10-100µm (Pradny et al., 2006; Prang et al., 2006). Theoretically, hydrogel is in a liquid state therefore no matter how the shape of cavity is, gel can fill cavities making use of its fluidity. Liquid state of gel

facilitates incorporating other agents or cell. Injection of injectable hydrogels in contusion SCI would not necessitate further damage since intact meninges are not disrupted by injection. Gelation phase in vivo can provide mechanical strength mimicking native tissue.

Only several studies have used injectable hydrogel for contusion injury model. One group demonstrated that injectable hydrogel (Hyaluronan and methylcellulose) could be employed in contusive injury model (Kang et al., 2013). Despite its positive effects on preservation of blood vessel density, it failed to completely bridge the cystic cavities developed after contusion injury (Austin et al., 2012; Mothe et al., 2013). To my knowledge, there is no study that reported successful bridging of cystic cavities in contusion injury model.

Among injectable hydrogels, temperature sensitive hydrogel is a advanced material since it has rapid sol-gel transition behavior and gelation occurs in situ at 37℃ (Jeong et al., 2002; Klouda and Mikos, 2008). Because the temperature-sensitive hydrogel can be maintained in a liquid state at low temperature, it is readily mixed with various soluble agents such as drugs, cells, trophic factors, enzyme, peptides, etc. Finally, gelation process would entail building up a mechanical framework that supports axon growth as well as creating a vital matrix that mimics ECM.

E. Aims of Study

Considering most suitable scaffold among various biomaterials with different advantages and disadvantages, characteristics of temperature sensitive injectable hydrogel seemed to be most optimal for the purpose of a bridging strategy in contusive spinal cord injury model. In my study, I examined potential beneficial effects of a temperature sensitive hydrogel, poly(phosphazene) hydrogel (I-5), in contusive spinal cord injury model and examined whether this bridging effect can bring out functional recovery.

II. MATERIALS AND METHODS

1. Animal and surgical procedures

Aldult female SpagueDawley rats (250-300g).All animal protocols were approved by the Institutional Animal Care and Use Committee of Ajou University School of Medicine. Rats were injected with 4% chloral hydrate to be anesthetized (10 ml/kg, injected intraperitoneally), followed by a dorsal laminectomy at the 10th thoracic vertebral level (T10-11) to expose the dorsal surface of the spinal cord. The IH Impactor was used to produce standardized contusion of 200 kdyn, muscles tissues were sutured in layer, and the skin was stapled.

2. Poly (phosphazene) hydrogel injection

For hydrogel injection, animals were randomly divided into 2 groups PBS (n=6) or poly(phosphazene) hydrogel (I-5) (n=6) was provided by Korean Institute of Science and Technology, 1 week after contusion spinal cord injury, rats were re-anesthetized and the lesion sites were exposed again, 8μl of PBS or hydrogel was injected manually using manual microliter Halmington syringe (model 701RN, USA). Before injection, gel was stored on ice to prevent gelation. After injection, needle was incubated in spinal cord lesion site for 30s to prevent overflow.

3. Tissue processing

For histological assessment of lesion site, animals were killed at 1 or 4 weeks after hydrogel or PBS injection (2 or 5 weeks after injury) for early and late time points. Spinal cord tissue was taken as previously described (Hwang et al., 2014). Animals were anesthetized with 4% chloral hydrate and perfused intracardially with PBS, followed by 4.0% paraformaldehyde in 0.1 M phosphate buffer, pH 7.4. Then, spinal cord was dissected and tissue block containing the epicenter ± 1 cm-long spinal cord was postfixed in 4.0 % paraformaldehyde for up to 6-8 hours, and then tissue was cryoprotected in a graded series of sucrose solutions. Sections of the spinal cord were cut transversely with 2 0 ε mnesst h i c k using a cryostat (CM 1900; Leica) and thaw-mounted onto Super Frost Plus slides (Fisher Scientific). Slides contain spinal cord samples were dry out at 35℃ for 1 hour and stored at -20℃ for further examination.

4. Immunohistochemistry

For immunohistochemistry, spinal cord tissue sections were incubated overnight at 4℃ with the following primary antibodies: anti-GFAP (1:500, chicken polyclonal, abcam), anti-fibronectin (1:100, rabbit polyclonal; Sigma), CS-56 (1:200, mouse monoclonal; Sigma), Iba-1 (1:500, rabbit polyclonal; Wako), anti-PDGFR-β (1:300, rabbit polyclonal; abcam). anti-collagen 1Ŭ1 (1:100, mouse monoclonal; Millipore), MMP-9, (1:100, rabbit polyclonal; Millipore), anti-CD45 (1:500, mouse; serotec), and anti-CD11b (1:500, mouse; Serotec) antibodies. After washing three times, slides were incubated with appropriate secondary antibodies conjugated to the Alexa Fluor fluorescent dyes. Images were taken using the Olympus confocal laser scanning microscope (model FV 300).

5. Three dimensional reconstruction of lesion cavity

For quantitative analysis of cavity volume, serial spinal cord sections stained with eriochrome and eosin were three-dimensionally reconstructed. For eriochrome and eosin staining, the cross sections of spinal cord were immersed for 8 min in a staining solution consisting of 240 ml of 0.2% eriochrome cyanine RC (Sigma) and 10 ml of 10% $FeCl_3 \cdot 6H_2O$ (Sigma) in 3% HCl. The sections were then washed with running tap water, followed by differentiation in 1% NH_4OH. After eriochrome cyanine staining, the sections were counterstained with eosin solution to visualize the entire spinal cord regions and lesion cavities clearly. Three dimensional reconstruction of lesion cavity was done using the Neurolucida Virtual Tissue 3D ver 10(MBF bioscience). Contours of the spinal cord outer boundary, white matter region, cystic cavity, and lesioned spinal cord tissue were manually drawn on each section, and the software generated 3D images. Different colors was assigned to distinguish white matter (white), grey matter (green), lesion (yellow), and cystic cavity (red). The volume of cystic cavities and residual tissue was was calculated automatically by the Neurolucida software.

6. Zymography

For the detection of activity of matrix metalloproteinase 2 and 9 (MMP-2 and MMM-9), PBS (N=5) and I-5 (N=4) injected animals were killed at 1 week after injection., 1 cm-long spinal cord segment with epicenter region at the center was freshly dissected and were quickly frozen at -80℃. The spinal cord tissue was homogenized and sonicated in

RIPA buffer containing 50 mM Tris-HCl, pH 8.0, 150 mM NaCl, 1% NP-40, 0.5% deoxycholate, and 1% SDS. Fifty µg protein from each sample was loaded onto a polyacrylamide gel containing SDS (to linearize the proteins) and gelatin (substrate for MMP-2 and MMP-9) and subjected to electrophoresis. Then, the gel was re-natured to allow proteins to regain their tertiary structure that is necessary for enzymatic activity by providing renaturing buffer (2.5% Triton X-100 and then incubated in substrate buffer (50 mM Tris-HCl, pH 8.5, 5 mM CaCl2) in 1hour followed by 3 times washing with developing buffer, 10 minute each time. Gels were transferred to fresh developing buffer (Tris base 50mM, NaCl 200mM, $ZnCl_2$, $CaCl_2.2H_20$ 5mM and NaN_3 0.02%) and incubate in 37℃ for 72 hours to allow the protease to digest its substrate. Then, the gel was stained by Comassi blue in 2 hours and then was destained in methanol and formic acid. After washing the excess dye off the gel, areas of protease digestion appear as clear bands. Band intensity between PBS and -I-5 group was determined by densitometry, using ImageJ software.

7. Behavioral assessment

For comparison of behavioral recovery, animals were randomly allocated to either PBS (N = 9) or hydrogel (N = 8) injection group after contusion injury. Locomotor recovery was evaluated using the Basso, Beattie and Bresnahan (BBB) open field locomotor scale and Catwalk footprint analysis. For BBB test, rats were allowed to walk freely in an open field and the BBB locomotor rating scale was determined after the 3-minute observation. Recovery of hindlimb movements was assessed 1 day after injury and then once a week for the duration of 8 weeks.

For the computerized footprint analysis, Catwalk system (Noldus Information Technology) was used. Animals were pretrained to walk on the Catwalk runway in an uninterrupted manner. On the test day, 4 runs with significant interruption were obtained. Individual footprints were determined manually using the Catwalk software (ver 7.1). Then, the software automatically calculated the following gait parameters: stride length, base of support, relative position and rotation angle. The angle of hindpaw rotation was defined as the angle (in degrees) of the hindpaw axis relative to the horizontal plane. Base of support was measured by the width between the left and right hindpaws. Left and right hindpaws were averaged to calculate the stride length and paw angle values. Footprints of hindpaws tend to overlap those of forepaws during walking in uninjured animals. However, injured

animals often lose this coordination between hind- and forepaws (Hamers et al., 2006). Therefore, relative position of fore- and hindpaws was obtained by directly measuring the distance between the center pads of fore- and hindpaws. Statistical analysis

Statistical analysis was performed with test or one-way ANOVA was used for comparison of group means. Repeated-measures two-way ANOVAs were used to compare differences in BBB scores matched at different time points. Error bars in all graphs represent standard error of mean (SEM).

III. RESULTS

1. Hydrogel injection prevent cavity formation after contusive spinal cord injury

Previous studies showed that discernable cystic cavities were formed as early as 1 week after spinal cord contusion injury. Cystic cavities were progressively enlarged by 4 week time point and there was no obvious difference between the 4 and 10-week time points (Ek et al., 2010). Based on this previous report, I chose to examine cavity formation at 4-week time points after injection of PBS or Hydrogel (I-5). Injection was performed 1 week after contusion injury, allowing cystic space to be formed to avoid potential tissue damages related to the injection itself. Cross sections of spinal cord tissues were stained with eriochrome and eosin dyes to distinguish myelinated areas (eriochrome, blue) and extracellular matrix (ECM) (eosin, pink) from the cystic cavities (no colors). As expected, a large cystic cavity was observed at the epicenter region of animals injected with PBS (Fig. 1B), extending rostrocaudally up to 1.2 mm away from the epicenter (Fig. 1A and Fig. 1C respectively). In contrast, virtually no cavity was found at the epicenter region of animals that received I-5 injection (Fig. 1D-F). Instead of cystic cavities, eosin-stained ECM-like tissue was observed at the central region.

To quantitatively compare cavity volumes between the two groups, cross-sectional images of the spinal cord were reconstructed to produce three-dimensional image using the Neurolucida software. I assigned different colors to different structures; red color for lesion cavity, yellow for remaining, but damaged tissue, green for remaining and intact gray matter, and gray for remaining white matter. As can be seen in the figure, cavity volume was sharply declined in animals with I-5 injection (Fig. 2B) compared to the large volume marked as cavity in PBS injected animals (Fig. 2A). Quantification data confirmed that the cavity volume in PBS group (mean = 1.460e+009 ± 5.150e+008 N=6) was significantly decreased compared to that of I-5 group (mean = 1.507e+008 ± 5.857e+007 N=6), resulting in the reduction of cavity volume to only 10% of control value by hydrogel injection (Fig. 2C). The volume of residual tissue was calculated by subtracting the cavity volume from the volume of entire, virtual spinal cord tissue limited by outer boundaries, PBS group (mean = 1.888e+010 ± 1.384e+009 N=6), I-5 group (mean = 2.333e+010 ± 1.164e+009 N=6). Quantification graph showed that spare tissue volume in hydrogel injected animals (mean =

$2.84x10^{10}$ μm^3) was also significantly greater than those in PBS group (Fig. 2D). In summary, I-5 injection virtually prevented formation of cystic cavities and contributed to the preservation of spinal cord tissue after contusion injury.

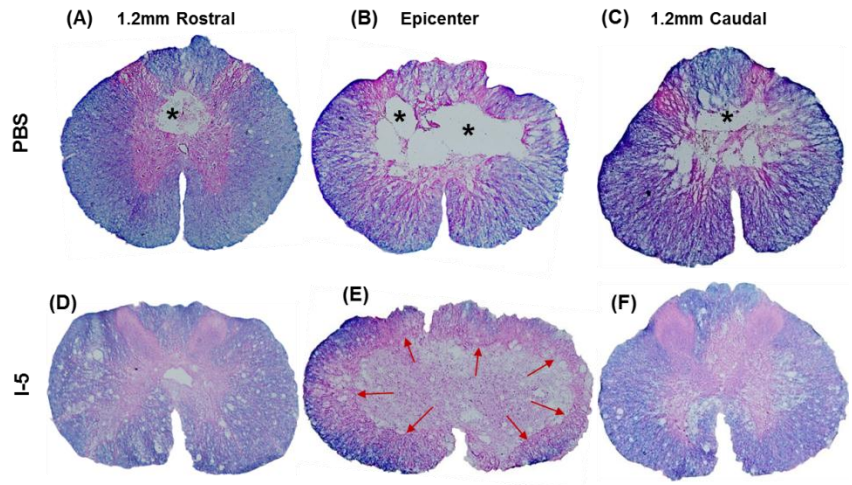

Figure 1. Eriochrome and Eosin staining of spinal cord cross sections 4 weeks after injection. (A-C) Representative images of transverse section of spinal cord tissue obtained from animals with PBS injection. (A) 1.2mm rostral to epicenter, (B) epicenter, (C) 1.2mm caudal to epicenter. (D-F) Representative images of transverse section of spinal cord tissue obtained from animals with hydrogel injection. (D) 1.2mm rostral to epicenter, (E) epicenter, (F) 1.2mm caudal to epicenter. Spinal cord sections were stained with eriochrome and eosin dyes. * injury cavity, red arrows: eosin-stained new matrix replacing cavity space.

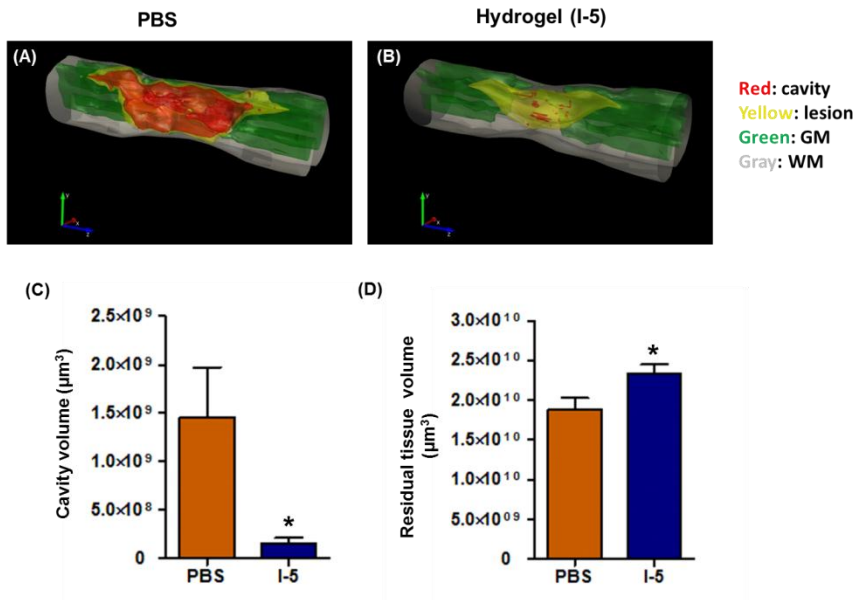

Figure 2. There dimensional reconstruction of lesion cavity. (A) 3D Image of PBS injected animal. (B) 3D image of hydrogel injected animal. Red: cavity, Yellow: lesion, Green: grey matter, Gray: white matter. (C) Quantification of cavity volume. Orange bar indicates PBS injected group (n=6), navy bar indicates I-5 injected group (n=6). Cavity volume was significantly reduced by one-tenth by hydrogel injection. (D) Quantification graph of residual tissue volume. In I-5 group, the volume of residual tissue was significantly higher that that of PBS group. (*****) represent $p < 0.05$ by unpaired t test.

2. Hydrogel injection suppress microglial activation 4 week after injection

Hydrogel is artificially generated foreign material. Upon introduction to spinal cord tissue, therefore, it is likely to evoke foreign body reactions comprising activation of inflammatory cells (Kang et al., 2010). To examine the possibility of exaggerated inflammtory activation, spinal cord sections obtained at 1 or 4 weeks after injection were immunostained with microglial marker, Iba1. At 1 week after injection, intense Iba1 positive signals were observed in and around the epicenter, to a similar extent in both groups (Fig. 3A and 3B). At 4 weeks after injection, Iba-1 positive signals seemed to be concentrated around lesion cavities with signal strength not apparently attenated compared to that at 1-week time point (Fig. 3E). In animals with hydrogel injection, Iba-1 postive signals were very weak in and around the areas with new matrix replacing cavity space onspicuous cavity space (Fig. 3F). Enlarged images of Iba1 showed that morphology and intensity of Iba1 possitive macrophages was similar between PBS and I-5 group at 1 week time point (Fig. 3C and 3D), respectively. Howerver, at 4 week time point, intensity of Iba1 macrophage in I-5 group was subsided dramatically (Fig. 3H) in comparison with that in PBS group. (n=6 each group). And then intensity was evaluated by Image J. The quantification graph from the data at 4-week time point showed that the intensity of Iba-1 positive signals were significantly decreased in hydrogel group (Fig. 3I). These data suggest that injected hydrogel did not provoke foreign body inflammatory reactions, rather the hydrogel suppressed injury-related activation of microglial cells.

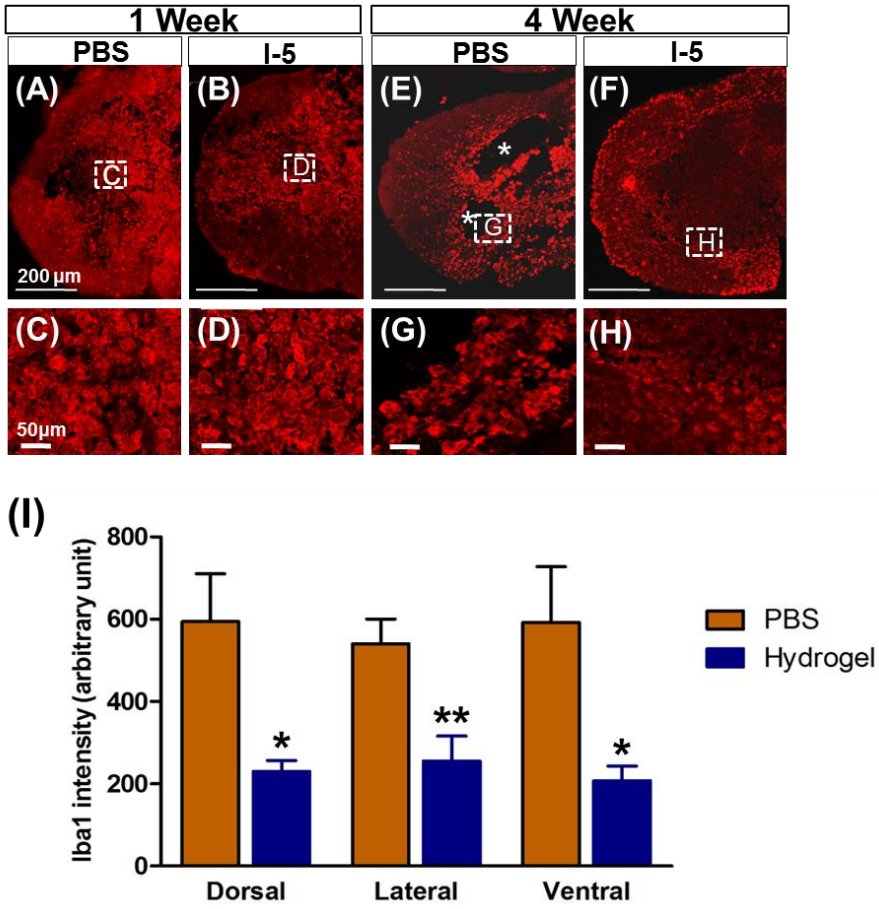

Figure 3. I-5 injection suppressed microglial activation. Injection of hydrogel significantly reduced microglial activation at 4 week after injection. Representative images of Iba1 possitive macrophages stained at 1 week (A-D) and 4 week (E-H) after injection of PBS (A, C, E, G) or hydrogel (B, D, F, H). (C, D, G, H) higher magnification images of boxed regions in (A, B, E, F), respectively. (I) Quantification graph of Iba1 intensity (arbitrary unit). PBS or I-5 group (N = 6 for each group). (*) and (**) represent $p < 0.05$ and $p < 0.01$, respectively, by *post hoc* analysis. (A, B, E, and F) Scale bars represent 200 µm, (C, D, G, and H) Scale bars represent 50 µm.

3. Remodelling of extracellular matrix by I-5 injection

Next, I sought to characterize the ECM deposited at the epicenter region where cystic cavity is supposed to be formed without I-5 injection. At 1 week after injection, GFAP immunostaining showed increased astroglial activity at the central area of the epicenter region and formation of cystic cavity seemed to begin at this time point in animals with PBS injection (Fig. 4A, D). Fibronectin (FN) immunostaining was performed simultaneously to examine deposition of fibroblast-derived matrix. FN-positive matrix was densly observed at the lesion center (Fig. 4B,E), but the FN-positive areas tended to be segregated from GFAP-positive regions (Fig. 4C). In animals with I-5 injection, denser and more extensive FN-positive matrix occupied the lesion center (Fig. 4G,I) and GFAP-positive astroglial acitvity seemed to be more clearly segregated compared to animals with PBS injection (Fig. 4F,H,J). Again, there was no evidence of cavity formation in this group. (Fig. 4F-J). At 4 weeks after injection, the majority of FN-positive matrix was replaced by cystic cavities formed at the lesion center in animals with PBS injection (Fig. 4M,N). GFAP-positive astrocytes were hardly observed in the FN-positive regions at this time point (Fig. 4K,L,O). In animals with I-5 injection, the FN-positive matrix seemed to be more concentrated and virtually occupied the entire central regions of the epicenter (Fig. 4Q,T). Segregation between GFAP-positive and FN-positive areas became solidifed at this time point, and there was a discrete boundary (white arrows in Fig. 4Q,R) between the matrix formed by GFAP-positive astrocytes and fibroblasts (Fig. 4P,R,S).

The above findings indicated that I-5 injection resulted in deposition of newly formed matrix derived from fibroblasts at the lesion epicenter, preventing formation of cytic cavities. This suggests that fibroblasts and fibroblastic scars may play a role in the I-5-induced deposition of matrix and abrogation of cavity formation. A previous study has demonstrated that microtubule stabilizer Taxol can reduce fibrotic scar. To examine if activity of fibroblast scars contributes to the I-5 effects in bridging cystic cavities, I mixed I-5 with Taxol (5μg) and injected the mixture into the injury site. Injection of I-5 mixed with Taxol resulted in the failure of the deposition of FN(+) matrix and the development of cystic cavities in the leion center (Fig. 5C,D), while this phenomenon did not occur in animals with I-5 injection only (Fig. 5A,B). This result suggested that deposition of FN-positive matrix

derived from fibroblasts is essential in the prevention of cystic cavity formation by I-5 injection.

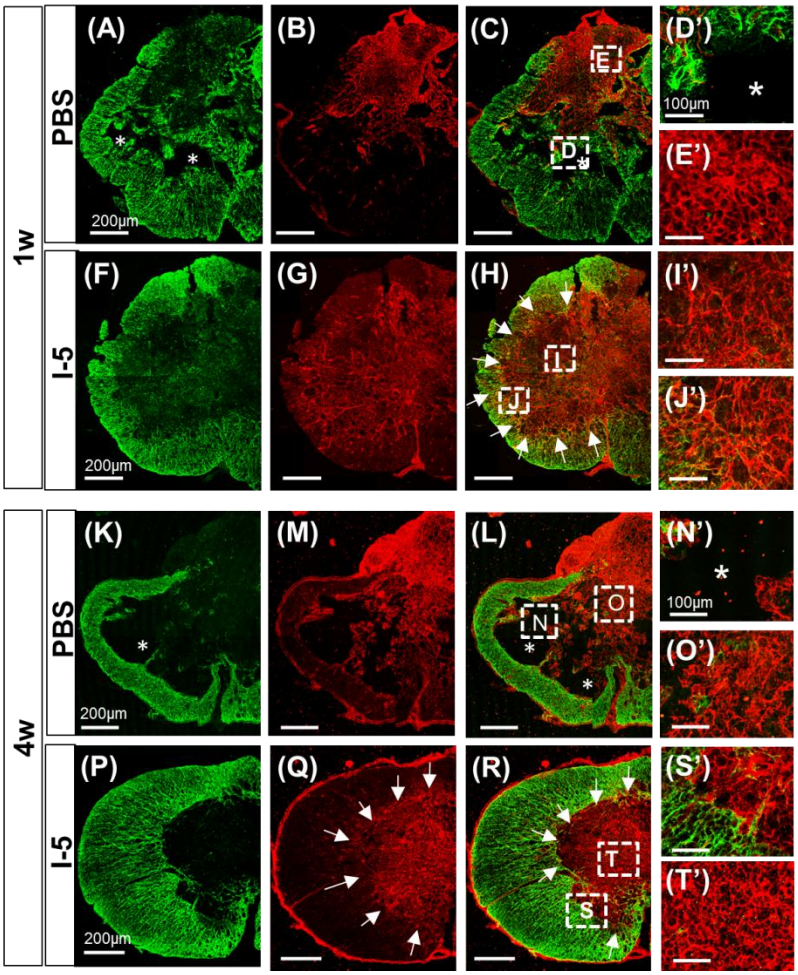

Figure 4. Remodelling of matrix by I-5 injection at 1 and 4 week. (A-J ô) Represen images at 1 week after injection. (A-E ô) Fibronectin possitive replaced by cavity spaces (*). (A) GFAP possitive astrocyte (green) confine the lesion site. (B) lesion core was occupied by FN(+) matr high magnification of (D) from (C) represe indicates FN(+) matrix. (K-O ô) 4 after PBS injection, most of FN (+) matrix was replaced by cavity spaces. (K) GFAP, (M) f image of (N) from (L) illustrate cavity. (FN(+) matrix. Scale bars from low magnification in (A) (B) (C) (F) (G) (H) (K) (M) (L) (P) (Q) (R) represent 200Õm. Scale bars in (Dô (A-C), (K-L).

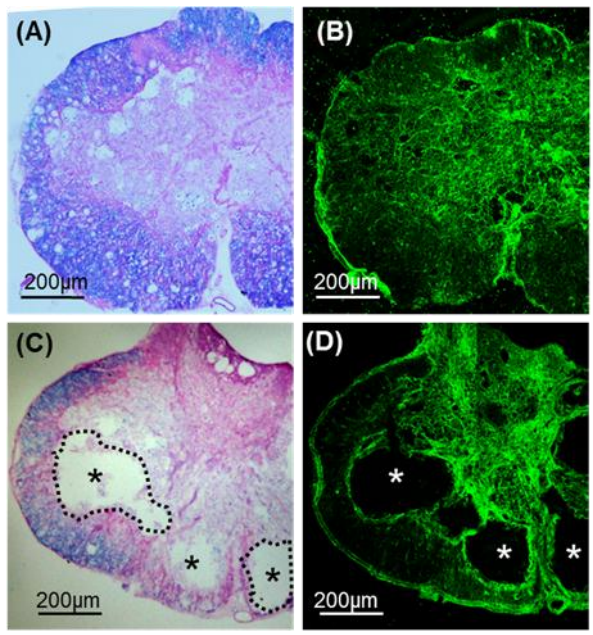

Figure 5. FN(+) matrix is essential in the prevention of cystic cavity formation by I-5. (A) (C) Representative image from I-5 injected spinal cord sections with or without Taxol administration. (A) Eriochrome and Eosin staining showed very little cavities. Myelin stained with Eriochrome (blue), Eosin stained ECM (pink). (B) (D) Sections stained with Fibronectin. Injection of I-5 mixed with Taxol failed to form FN(+) matrix. (*) indicates cavities, dotted circles represent boundary between cavity and residual tissue. All scale bars represent 200μm.

4. Matrixmetallo-proteinase-9 (MMP-9) involved in ECM remodelling

The above results suggested that hydrogel injection may induce remodeling of ECM leading to prevention of cavitation and deposition of fibroblast-derived matrix. I hypothesized that ECM remodeling enzyme matrixmetalloproteinase (MMP) is invovled in this process. MMPs are zinc-endopeptidase with multiple functions involved in both pathological and physical conditions in CNS. Of all the MMP family members, MMP-9 and MMP-2 belong to gelatinase familly (Zhang et al., 2011). There is increasing evidence that gelatinase activity has benifical role in matrix remodelling and wound healing (Hsu et al., 2006; Kyriakides et al., 2009). I performed gelatinase zymography to detect gelatinase activity using spinal cord lysates obtained 1 week after injection of PBS or I-5. Compared to animals with PBS injection, MMP-9 activity was clearly enhanced in animals with hydrogel injection. Quantification graph showed that mean intensity of MMP-9 band was 7.1 ± 0.4732 N=5 in PBS groups and 16.15 ± 1.531 N=4 in I-5 group, which was 2-fold increase compared to PBS group (Fig. 6L). Quantification graph demonstrated that MMP-9 activity in I-5 group significantly surged.

I also performed immunohistochemistry to examine cellular sources for MMP-9 acitvity. As expected, MMP-9 immunoreactivity was elevated within FN-positive matrix in animals with I-5 injection (Fig. 6D-F). In contrast, there was no discernable MMP-9 immunoreactivity in remaining FN-positive matrix in animals with PBS injection (Fig. 6A-C). The majority of MMP-9 immunoreactivity was colocalized with CD11b immunoreactivity, indicating that MMP-9 was predominantly expression in macrophage or microglial cells within FN-positive matrix.